Delineation of Mangroves in Lothian, Sundarbans using multi-frequency SAR and Optical Remote Sensing

Nilima R. Chaube[1], Yashraj Jain[2]

1. Scientist/Engineer-SG, DQCG / SIPA, Space Application Centre (ISRO), Ahmedabad, 380015, Gujarat, India
2. Junior Research Fellow, Computer Engineering Department, IITE, Indus University, Ahmedabad, 382115, Gujarat, India
Contributing Authors: chaube@sac.isro.gov.in, yashraj7196@gmail.com

Keywords: ALOS PALSAR, Sentinel – 1, Sentinel – 2 MSI, Mangrove Vegetation Index (MVI), Normalized Difference Vegetation Index (NDVI), Mangrove Forest

Abstract

Mangrove ecosystems play a crucial role in coastal biodiversity, carbon sequestration, and shoreline stabilization. Delineating mangrove and non-mangrove areas accurately remains a challenge using remote sensing data due to its presence in dynamic intertidal ocean and tidal wave variability. The present study brings out the wetland discrimination capability of ALOS PALSAR-2 (L-band), NovaSAR-1 (S-band), Sentinel-1 (C-band), and Sentinel-2 MSI using Support Vector Machine (SVM) classification.
The classification results using SAR, Sentinel-1 (C-band) achieved an overall accuracy of 91.1104% with a kappa coefficient of 0.8277, better than ALOS PALSAR-2 (L-band) and NovaSAR-1 (S-band). The better classification accuracy of 96.39% with kappa coefficient 0.92 is achieved with combination of L, C SAR and Sentinel-2 MVI data due to sensitivity of SAR to forest structure and moisture. The mangrove extent obtained through optical NDVI and MVI data is overestimated due to different approach of these vegetation index. The mangrove extent is overestimated using multi-band combination of SAR 38.6 sq km and SAR-Optical combination 39.62 sq km as compared to 31.06 sq km estimated by Global Mangrove Watch (GMW) in year 2020 and 30.00 km² in Forest Survey of India (FSI) 2021 report for Lothian, Sundarbans.
The study highlights that classification using multi-frequency-polarization SAR and cloud free optical imagery stacked with SAR data have advantage in frequently cloud covered study area. This research contributes to coastal resource management and conservation, for large-scale mangrove monitoring. Future studies should explore deep learning approaches and time-series analysis to improve the long-term sustainability of these critical ecosystems.

1. Introduction

Mangrove forests play a vital role in supporting coastal livelihoods by providing essential ecosystem services such as fisheries, wood for fuel and construction, and coastal protection, which contribute to the economic and social well-being of local communities. Their dense root systems act as natural barriers against storm surges and coastal erosion, safeguarding inland settlements and agricultural lands (Gupta et al., 2018) and (Kuenzer et al., 2011). However, the inaccessibility of many mangrove areas due to their location in intertidal zones, dense vegetation, and muddy substrates poses challenges for resource extraction, monitoring, and conservation efforts (Baloloy et al., 2020). Accurate geographical information on the extent and health of mangrove forests is essential for effective land-use planning and natural resource management, ensuring sustainable development and biodiversity conservation in coastal regions (Snedaker, 1982) and (Lugo and Snedaker, 1974). Remote sensing technologies and geospatial analyses have become indispensable tools in addressing these challenges, providing reliable data for decision-making and policy formulation.

According to age and location, the mangrove vegetation has an evergreen, basic physiognomic structure with two to three levels that range in height from 5 to 25 m (MacNae, 1968), (Tomlinson, 1986), (Ball, 1988), (Clough, 1992), (Chapman, 1975), (Duke, 1992), and (Smith, 1992).

Remote sensing has emerged as a widely used technology for mapping mangrove forests, offering an efficient and cost-effective alternative to field-based approaches, which are often limited to local-scale assessments (FAO, 2003) and (Spalding et al., 1997). This technology enables scientists and planners to monitor and analyze true changes in the areal extent and spatial structure of mangrove forests over time.

The objective of this research is to delineate mangrove and non-mangrove areas using multi-frequency microwave & multi-band optical data. SAR data is used in separately & stacked together the Support Vector Machine (SVM) algorithm, a supervised machine learning approach. This study aims to apply the Normalized Difference Vegetation Index (NDVI) and Mangrove Vegetation Index (MVI) with Land Use and Land Cover (LULC) classification to accurately differentiate mangrove forests from other land cover types. This research aims to enhance the accuracy and reliability of mangrove mapping, contributing to improved coastal ecosystem monitoring and management.

2. Study Area

https://doi.org/10.5194/isprs-archives-XLIX-B3-2026-923-2026

Lothian Island, situated within the Indian Sundarbans in the South 24 Parganas district of West Bengal, represents a significant mangrove-dominated landscape. The island is geographically positioned at 21°34'45" N latitude and 88°16'06" E longitude and spans approximately 38 km². Lothian Island is primarily formed from sediment deposits brought by the Ganges River, leading to an average elevation of about 3 meters above sea level. The climatic conditions on the island exhibit seasonal variations, with winter temperatures ranging between 2°C and 4°C, while summer temperatures can reach as high as 43°C in March (Hati et al., 2022). The region receives an annual average rainfall of 1,661.6 mm, with the majority of precipitation occurring during the southwest monsoon season (Gopal and Chauhan, 2006).

Figure 1 provides a detailed visual representation of the Lothian region within the Sundarbans, highlighting the distribution of ground truth locations collected for mangrove classification and validation. The map integrates high-resolution Google Earth imagery with ground truth data points, serving as a crucial reference for assessing mangrove extent and spatial distribution. These ground truth locations are essential for validating remote sensing-based classification techniques, ensuring accuracy in delineating mangrove and non-mangrove regions.

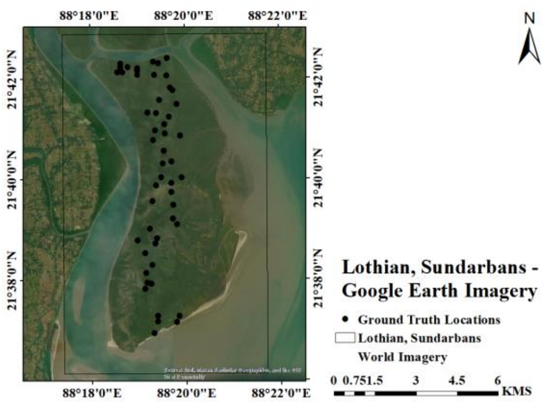

Figure 1. Mangroves study region of Lothian, Sundarbans with ground truth locations

3. Datasets Used

In this study, multiple remote sensing datasets from different satellite sensors were utilized to accurately delineate mangrove and non-mangrove areas using a combination of optical and synthetic aperture radar (SAR) data. The datasets include SAR-based observations from ALOS PALSAR-2 (L-band), Sentinel-1 (C-band), and NovaSAR-1 (S-band), as well as multispectral data from Sentinel-2 MSI. Table 1 illustrates the different specifications of the data used in this study.

S. No.	Data Products (Resolution)	Sensors / Frequency Band	Date of Acquisition	Polarization / Bands	Central Incidence Angle
1	Global yearly mosaic - JAXA (25m)	ALOS PALSAR 1 & 2 - L band	2020 yearly mosaic	HH+HV (Fine Beam Dual - pol data)	38.382 (near range) & 42.561 (far range)
2	Level - 1 GRD - ESA (10m)	Sentinel - 1 - SAR - C band	15-03-2021	VV + VH (SAR Standard High resolution Dual - pol data)	30.830 (near range) & 46.088 (far range)
3	Multispectral Instrument - ESA (10m)	Sentinel - 2 MSI	29 - 02 - 2020	13 bands - spanning from the Visible and Near Infra-Red (VNIR) to the Short Wave Infra - Red (SWIR)	Mean viewing incidence angle a. Zenith angle varying b/w 2.559° to 3.30° b. Azimuth angle varying b/w 152.89° to 159.11°
4	Dual Pol - ScanSAR - ESA (20m)	NovaSAR - 1	26 - 05 - 2021	VV and HH (Scan SAR mode)	28.48

Table 1. Data specifications of different Sensors

4. Methodology

The methodology employed in this study integrates synthetic aperture radar (SAR) datasets and multispectral optical datasets to accurately delineate mangrove and non-mangrove areas in the Lothian region of the Sundarbans. The process consists of data pre-processing, vegetation index computation, machine learning-based classification, accuracy assessment, and classified map generation, as illustrated in Figure 2.

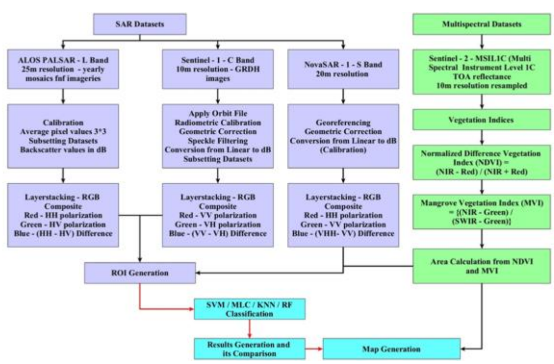

Figure 2. Flow chart showing methodology followed for Mangroves and Non-mangroves delineation for Lothian, Sundarbans

This study employs a combination of synthetic aperture radar (SAR) and multispectral optical datasets to accurately delineate mangrove and non-mangrove areas in the Lothian region of the Sundarbans. The classification process leverages SAR backscatter properties, vegetation indices, and supervised machine learning techniques to achieve high accuracy in land cover classification. The SAR datasets provide insights into vegetation structure as L, S and C band has different penetration, density, and water content in mangrove forest.

Sentinel-2 MSI (10m resolution) optical image is pre-processed by converting raw radiance values to Top-of-Atmosphere (TOA) reflectance. Two vegetation indices, Normalized Difference Vegetation Index (NDVI) & Mangrove Vegetation Index (MVI) are computed for further analysis. The NDVI is used to assess general vegetation health while MVI enhances the presence of mangrove based on unique spectral properties.

The classification process involved generating Regions of Interest (ROIs) from both SAR and multispectral datasets to create training samples for classification models. The Support Vector Machine (SVM) is selected as the preferred classification technique due to its ability to handle complex spectral variability within mangrove and non-mangrove regions. The classification results are evaluated through confusion matrix analysis, Kappa coefficient calculation, and overall accuracy assessment to determine the best-performing approach. Once validated, a mangrove and non-mangrove map was generated, depicting the spatial distribution of mangrove forests in the Lothian region of the Sundarbans.

4.1 Satellite Data Preprocessing

Before radiometric calibration, pre-processing involves updating satellite data such as satellite, satellite velocity using an orbit file. Sigma-0 data in decibels (dB) converted from Digital Numbers (DN) data using the equation 1, where CF is the calibration factor listed in corresponding metadata file. The imagery projected to WGS-1984, and the backscatter data is geocoded.

$$\sigma^\circ \, (dB) = 20 * \log 10 \, (DN) + CF \quad (1)$$

The speckle free averaged pixel values obtained after applying Lee filter of kernel size of 3 * 3. A RGB composite created by co, cross and difference of polarization of each sensor.

4.2 Vegetation Indices

Vegetation Indices (VIs) are multi-wavelength surface reflectance combinations that highlight a particular characteristic of vegetation. Each VI aims to draw attention to a particular plant characteristic. The study used the following Vegetation Indices (VIs):

4.2.1 Normalized Difference Vegetation Index (NDVI)

Healthy vegetation has a spectral signature that shows a sharp peak in the level of reflection at 0.7 m, but un-vegetated land has a consistent linear course depending on the kind of surface. The near infrared (0.78 to 1 m) reflectance intensity is a measure of how active a plant's chlorophyll is. NDVI is estimated using equation 2.

$$NDVI = (NIR - Red) / (NIR + Red) = (Band8 - Band4) / (Band8 + Band4) \quad (2)$$

Where, NIR = Near Infrared = Band8 (0.842μm) and Red = Band4 (0.665μm) of Sentinel-2.

4.2.2 Mangrove Vegetation Index (MVI)

The Mangrove Vegetation Index (MVI) is fit to map mangroves quickly and accurately without the need for labor-intensive and user-skill-biased complicated categorization algorithms (Baloloy et al., 2020). Mangrove pixels are distinguished from other non-vegetation cover, such as bare soil, water, and built-up areas, by the index' ability to capture their distinctive greenness and moisture content.

$$MVI = (NIR - Green) / (SWIR1 - Green) = (Band8 - Band3) / (Band11 - Band3) \quad (3)$$

Where, NIR, Green, and SWIR1 are the reflectance levels in bands 8 (0.842 m), 3 (0.559 m), and 11 (1.610 m) of Sentinel-2, respectively.

The first part of the equation, NIR-Green, underlines how the greenness of mangrove forests and terrestrial vegetation differ in different ways, while the second part, SWIR1-Green, illustrates how mangroves are particularly wet due to their surroundings. MVI is estimated using equation 3.

4.3 Classification Techniques

In this study, the Support Vector Machine (SVM) classification algorithm is employed for the accurate delineation of mangrove and non-mangrove areas. The fundamental principle of SVM is to construct an optimal hyperplane that maximizes the margin of separation between different land cover classes. The support vectors, which are the closest data points to the hyperplane, play a crucial role in defining the boundary. SVM is particularly advantageous for classifying remote sensing images as it effectively handles non-linearly separable data, reducing the impact of noise and spectral variability commonly found in SAR and multispectral imagery. The SAR dataset was categorized into four major classes: mangroves, non-mangrove vegetation, built-up areas, and ocean, while the Sentinel-2 multispectral dataset was classified into six categories: mangroves, ocean, vegetation (non-mangrove), built-up areas, mudflats, and unclassified regions.

The SVM classifier is trained using Regions of Interest (ROIs) created from field data and reference imagery. A Gaussian Radial Basis Function (RBF) kernel is applied to handle the complex spectral variations of mangrove forests and their surrounding land cover types. The classification results are validated using confusion matrix analysis, Kappa coefficient computation, and overall accuracy assessment to ensure reliability.

4.4 Results and Discussions

4.4.1 SAR and Optical Imageries Based Classification

Sentinel-1, SAR C-band RGB composite (VV, VH, VV - VH), ALOS PALSAR-2 L-band RGB composite (HH, HV, HH - HV), NovaSAR S-band RGB and registered composites of co-cross polarizations for L, S, C-band together are classified using SVM. These dual-polarized SAR datasets provide essential structural and backscatter properties for identifying mangrove canopies, intertidal zones, and water bodies. The integration of optical and SAR data further enhanced the classification.

The Figures 3, 4, 5, 6, 7, and 8 illustrates the classification outputs, highlighting the spatial distribution of mangroves, seawater, vegetation, and mudflats across the study region for SAR, Optical and combined Data. Sensitivity of L-band and C-band is for vegetation structure and canopy as depicted in Figure 3 and Figure 4. The classification using ALOS PALSAR (L-band) data (Figure 3) reveals that the seawater class often merges with the mudflat & other vegetation, leading to misclassification due to low backscatter contrast between water and dense vegetation in L-band SAR imagery, which limits its ability to accurately segment aquatic regions. Sentinel-1 (C-band) classification (Figure 4) shows a notable confusion between mudflats and mangroves, where mudflat areas are misclassified as mangrove forests due to the similar backscatter responses of wet soil and mangrove-dominated intertidal zones. Figure 5 shows poor delineation of mudflat, other vegetation & mangrove for S-band. S-band SAR lacks the necessary backscatter contrast to fully separate wetland classes. The classification results indicate that the Single band SAR-based classification results show limitations in distinguishing mangroves from other land cover types, mainly due to band backscatter are influenced by factors such as canopy structure, tree density, and moisture content, which do not always distinctly separate mangroves from terrestrial vegetation. These findings highlight the importance of integrating multispectral optical datasets with SAR data to enhance classification accuracy as shown in Figure 6. Due to registration issue, S-band

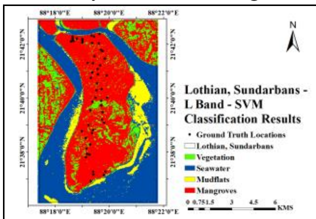

Figure 3. L-band

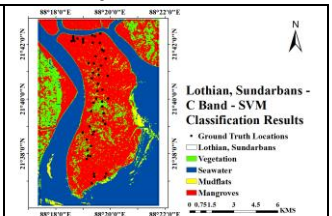

Figure 4. C-band

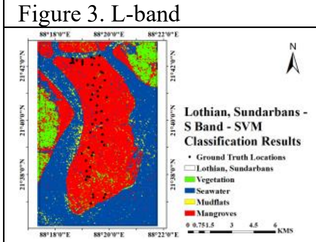

Figure 5. S-band

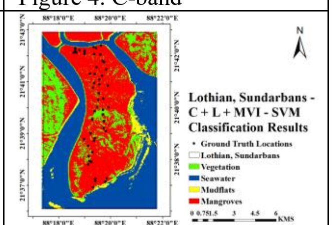

Figure 6. SAR+Optical

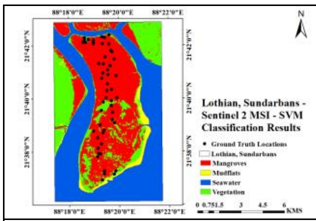

Figure 7. Sentinel-2 MSI

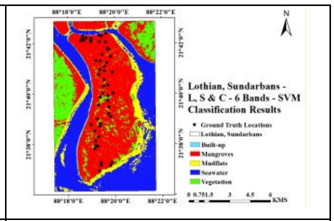

Figure 8. L + S + C

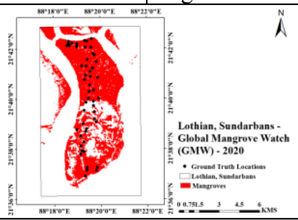

Figure 9. GMW Year 2020

data is not taken for SAR and Optical combined classification. Figure 7 depicts classification using Sentinel-2 MSI which has overestimated the terrestrial vegetation in green colour. Figure 8 depicts classification of multi frequency SAR data which has better wetland classification even with S-band registration issue. These classified outputs are validated against ground GMW mangrove extent for year 2020 as shown in Figure 9 and ground truth data points on Google Earth imagery depicted in Figure 1. The comparison of various combination confirms the effectiveness of SVM classification in mapping mangrove distributions in the Lothian Sundarbans.

The classification results from different sensors are presented in Table 2. The evaluation is based on overall accuracy, kappa coefficient, producer’s accuracy, user’s accuracy, and estimated mangrove area. The results indicate that multispectral optical classification using Sentinel-2 MSI and combined with SAR (L, C and MSI) produced higher accuracy, whereas individual SAR bands exhibited variations in accuracy due to sensor-specific limitations.

The highest accuracy (97.41%) achieved by combining L, S, and C bands, showing the advantage of multi-frequency SAR integration. Visually better result is obtained by combining L, C band & Sentinel-2 MSI. Among individual SAR frequencies, Sentinel-1 (C-band) classification (91.1104%) performed better than ALOS PALSAR-2 (L-band) (85.9289%) and NovaSAR-1 (S-band) (83.0612%), suggesting that C-band SAR is more effective in detecting canopy structures. The Kappa coefficient values further confirm these findings, with L, S, and C band integration (0.9622) and L, C & Sentinel-2 MSI (0.94), while L-band and S-band individually showed lower Kappa values (0.7372 and 0.6552, respectively).

S. No.	Parameters	L Band %	C Band %	S Band %	Sentinel-2 MSI	L+C+MSI	L+S+C
1	Overall Accuracy	85.92	91.11	83.06	96.96	96.39	97.41
2	Kappa Coeff.	0.73	0.82	0.65	0.95	0.92	0.96

3	Mangrove Producers Accuracy	90.13	88.90	95.89	100	94.44	97.21
4	Mangrove Users Accuracy	60.90	63.71	61.40	88.46	80.95	95.27
5	Mangrove Area in sq. kms.	42.40	42.30	43.06	33.14	39.62	38.60

Table 2: Results achieved from Classification

4.4.2 NDVI & MVI over Lothian

NDVI is a generalized vegetation index that measures vegetation greenness, making it sensitive to both mangroves and other vegetated regions such as mudflats, shrubs, and transitional intertidal zones.

MVI is a targeted vegetation index specifically designed for mangrove identification by leveraging the high moisture content and spectral reflectance of mangroves in the NIR, Green, and SWIR bands. The lower estimate suggests that some mangrove patches, particularly degraded or sparsely vegetated ones, may not have been fully captured using MVI due to spectral overlap with other vegetation types or highly waterlogged conditions.

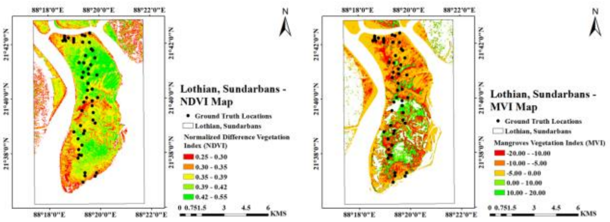

Figure 10. NDVI and MVI over Lothian, Sundarbans

Figure 10 illustrates NDVI and MVI variation over study area, since NDVI alone cannot fully distinguish mangroves from other vegetation types, the Mangrove Vegetation Index (MVI) is incorporated to enhance the mangrove area estimation. The total mangrove and vegetated area delineated using NDVI analysis is estimated to be 37.31 square kilometres, reflecting the extent of healthy and continuous vegetation patches in the study area. the NDVI-derived area appears higher by 7.31 square kilometres. This discrepancy could be attributed to the spectral characteristics of NDVI. The total mangrove-covered area estimated from MVI classification is 35.50 square kilometers, whereas the Forest Survey of India (FSI) report of 2021 estimates the mangrove area at approximately 30 square kilometers. The 5.50 square kilometer discrepancy between the two results suggests that MVI classification may have overestimated some mangrove regions, potentially due to spectral overlap with adjacent vegetation or incorrect exclusion of mangroves located in highly waterlogged or degraded areas.
The tidal information for Lothian from the nearby Sagar & Namkhana islands is provided in the Table 3. Sentinel – 1 (C band) sensor acquired data during high tide and Sentinel-2 MSI captured data during low tide.

S. No.	Data Product / Date of acquisition	Location (Tide time / height)		Tide type
		Sagar Island	Namkhana	
1	Level – 1 GRD – ESA - Sentinel – 1 – SAR - C band acquired on 15 - 03 - 2021	11:55 h / 4.2m	11:43 h / 4.7m	High
2	Multispectral Instrument – ESA - Sentinel – 2 MSI Optical acquired on 29 - 02 - 2020	7:30 h / 0.8m	7:54 h / 0.9m	Low

Table 3: Tidal Information for the acquired satellite images

The total mangrove area estimates derived from classification across different datasets is towards higher side. The highest estimated mangrove area (43.06 km²) is obtained from NovaSAR-1 (S-band) classification, indicating possible overestimation due to merging of mangroves with terrestrial vegetation. Conversely, Sentinel-1 (C-band) over estimated mangrove area (42.30 km²) even with its sensitivity to canopy. While a mangrove coverage of 30.00 km² for Lothian, Sundarbans is reported in Forest Survey of India (FSI) report (FSI, 2022) and 31.06 sq km from Global Mangrove Watch (GMW) year 2020 (Bunting et al., 2022).

C-band SAR is highly sensitive to canopy structure, but it sometimes underestimates mangrove extent in mixed vegetation areas, leading to slightly lower area estimations. S-band SAR’s sensitivity to surface roughness, which can cause mudflats and intertidal areas to be misclassified as mangroves. L-band SAR is effective for penetrating dense canopies, making it useful for distinguishing mangroves from other vegetation, though it may still merge some vegetation types due to similar backscatter responses. This study suggests that multi-frequency multi-polarization SAR integration helps to reduce misclassification errors, enhancing mangrove detection accuracy by capturing both canopy structure (C-band), penetration depth (L-band), and surface roughness (S-band). Also, combination of SAR and cloud free Optical data can give better delineation.

5. Conclusions

This study successfully demonstrates the application of multi-sensor remote sensing data for the delineation of mangrove and non-mangrove in the Lothian region of the Sundarbans. The variation in mangrove area estimates from different frequency data highlights the strengths and limitations of respective frequency. The FSI 2021 mangrove area of 30.00 km² is taken as baseline reference. NDVI and MVI value based mangrove area estimation is 37.31 and 35.50 square kilometers respectively, reflecting the overestimation as extent of healthy and continuous vegetation patches in the study area. Area is overestimated by Sentinel-1 C-band SAR classification as 42.30 km², L-band SAR as 42.40 km² and integrated multi-frequency SAR as 38.60 km². The Sentinel-2 MSI-based estimated area 33.14 km² closer to reference, shows the potential of optical remote sensing in mangrove ecosystem monitoring.

https://doi.org/10.5194/isprs-archives-XLIX-B3-2026-923-2026

Combination of SAR and MSI delineated wetland effectively but overestimated mangrove area ~ 39 sq km. The tide information is not considered in this study.

The SVM classification approach was highly effective in distinguishing mangroves from other land cover types, outperforming traditional classification methods. The combination of Sentinel-2 MSI and SAR data gives better mangrove classification, given its ability to capture spectral differences in vegetation. However, SAR is essential in areas affected by persistent cloud cover for monitoring vegetation structure and biomass changes.

The SVM classification accuracy assessment revealed that combination of Sentinel-2 MSI and SAR produced the overall accuracy more than 96%. Sentinel-1 C-band (91.1104%) exhibited better performance compared to ALOS PALSAR-2 L-band (85.9289%) and NovaSAR-1 S-band (83.0612%), showing that C-band SAR is more effective in capturing mangrove canopy characteristics.

The findings emphasize the importance of integrating multi-frequency-polarization SAR and SAR with optical datasets to enhance classification accuracy, as each dataset offers complementary strengths. SAR datasets are valuable for structural analysis, while optical datasets are more effective for spectral discrimination. This study provides a scientifically validated framework for large-scale mangrove classification, contributing to coastal conservation, climate change mitigation, and sustainable land-use planning. The results can support policy decisions aimed at protecting mangrove ecosystems in the Sundarbans and other similar coastal regions worldwide. The integration of multi-sensor remote sensing with machine learning ensures a repeatable and scalable methodology, offering a reliable tool for long-term monitoring and conservation of mangrove forests. Future research should explore deep learning-based classification techniques and time-series analysis to further improve mangrove mapping and change detection. Additionally, higher-resolution SAR and hyperspectral datasets could enhance classification precision, particularly for detecting small-scale mangrove degradation and seasonal changes in mangrove ecosystems.

6. Acknowledgement

This work is carried out under the project "Study of Mangroves using remote sensing data over Lothian, Sundarbans" sponsored by Space Application Centre, ISRO, Ahmedabad.

7. Declaration

There is no conflict of interest between the authors.

References

Ball, M. C., 1988. Ecophysiology of Mangrove. *Trees*, 2, 129–142.

Baloloy, A. B., Blanco, A. C., Sta. Ana, R. R. C., & Nadaoka, K., 2020. Development and application of a new mangrove vegetation index (MVI) for rapid and accurate mangrove mapping. *ISPRS Journal of Photogrammetry and Remote Sensing,* 166, 95–117. https://doi.org/10.1016/j.isprsjprs.2020.06.001

Bunting, P., Rosenqvist, A., Hilarides, L., Lucas, R., Thomas, N., Tadono, T., Worthington, T., Spalding, M., Murray, N., & Rebelo, L.-M., 2022. Global Mangrove Watch (1996 - 2020) Version 3.0 Dataset (3.0) [Data set]. Zenodo. https://doi.org/10.5281/zenodo.6894273

Chapman, V. J., 1975. *Mangrove Vegetation*. In: Cramer J CVJ (eds) (1977) Ecosystems of the world: wet ecosystems vol 1. Elsevier, New York.

Clough, B. F., 1992. Primary Productivity and Growth of Mangrove Forests. In A. I. Robertson, & D. M. Alongi (Eds.), *Tropical Mangrove Ecosystem, Coastal and Estuarine Studies* (pp. 225-250). American Geophysical Union.

Duke, N. C., 1992. Mangrove floristics and biogeography. In *Tropical Mangrove Ecosystems* (pp. 63-100).

FAO, 2003. Status and trends in mangrove area extent worldwide. *Forest Resources Assessment Working Paper No. 63.* Food and Agriculture Organization of the United Nations.

Forest Survey of India (FSI), 2022. India State of Forest Report 2021. Ministry of Environment, Forest and Climate Change, Government of India. https://fsi.nic.in/forest-report-2021-details

Gopal, B., & Chauhan, M., 2006. Biodiversity and its conservation in the Sundarbans mangrove ecosystem. *Aquatic Sciences*, 68(3), 338-354.

Gupta, Kaushik, Anirban Mukhopadhyay, Sandip Giri, Abhra Chanda, Sayani Datta Majumdar, Sourav Samanta, Debasish Mitra, Rabindro N. Samal, Ajit K. Pattnaik, and Sugata Hazra, 2018, "An Index for Discrimination of Mangroves from Non-Mangroves Using LANDSAT 8 OLI Imagery." Methods X5 (2018): 1129–39. https://doi.org/10.1016/j.mex.2018.09.011.

Hati, K. M., Mandal, S., Bandyopadhyay, P. K., & Sarkar, D., 2022. Environmental changes and their impacts on Sundarbans mangroves. *Environmental Monitoring and Assessment*, 194(5), 321.

Kuenzer, Claudia, Andrea Bluemel, Steffen Gebhardt, Tuan VO Quoc, and Stefan Dech, 2011. "Remote Sensing of Mangrove Ecosystems: A Review." *Remote Sensing* 3(5):878–928. Doi: 10.3390/rs3050878.

Lugo, A. E., & Snedaker, S. C., 1974. The Ecology of Mangroves. Annual Review of Ecology and Systematics, 5, 39-64. http://dx.doi.org/10.1146/annurev.es.05.110174.000351

MacNae, W., 1968. A General Account of the Fauna and Flora of Mangrove Swamps and Forests in the Indo-West-Pacific Region. *Advances in Marine Biology*, 6, 73–270.

Smith, T. J., III., 1992. Forest structure. In *Tropical Mangrove Ecosystems* (pp. 101-136)

Snedaker, S.C., 1982. Mangrove species zonation: why?. In: Sen, D.N., Rajpurohit, K.S. (eds) Contributions to the ecology of halophytes. Tasks for vegetation science, vol 2. Springer, Dordrecht. https://doi.org/10.1007/978-94-009-8037-2_8

Spalding, M., Blasco, F., & Field, C. D., 1997. World mangrove atlas. The International Society for Mangrove Ecosystems (ISME).

Tomlinson, P. B., 1986. *The Botany of Mangroves*. Cambridge tropical biology series, Cambridge University Press, pp 413